Early cognitive, structural and microstructural changes in c9orf72 presymptomatic carriers before 40 years of age

Anne Bertrand, Junhao Wen, Daisy Rinaldi, Marion Houot, Sabrina Sayah, Agnès Camuzat, Clémence Fournier, Sabrina Fontanella, Alexandre Routier, Philippe Couratier, et al.

Early cognitive, structural and microstructural changes in *c9orf72* presymptomatic carriers before 40 years of age

Anne Bertrand, MD, PhD[1,2,3,4]*, Junhao Wen, MS[2,5]*, Daisy Rinaldi, PhD[1,15], Marion Houot, MS[14], Sabrina Sayah, MS[5], Agnès Camuzat, PhD[5], Clémence Fournier, PhD[5], Sabrina Fontanella, MS[2,5], Alexandre Routier, MS[2,5], Philippe Couratier, MD[6], Florence Pasquier, MD PhD[7,8], Marie-Odile Habert, MD[9,10], Didier Hannequin, MD, PhD[11,12], Olivier Martinaud, MD, PhD[11,12], Paola Caroppo, MD, PhD[5,13], Richard Levy, MD, PhD[1,14,15]; Bruno Dubois, MD[1,14,15], Alexis Brice, MD[1], Stanley Durrleman, PhD[2,5], Olivier Colliot, PhD[1,2,16], Isabelle Le Ber, MD, PhD[1,14,15] and PREVDEMALS Study Group.

[1] Sorbonne Universités, UPMC Univ Paris 06, Inserm, CNRS, Institut du cerveau et la moelle (ICM), Assistance Publique-Hôpitaux de Paris (AP-HP) - Hôpital Pitié-Salpêtrière, Paris, France.

[2] Inria Paris, Aramis project-team, Paris, France.

[3] AP-HP, Hôpital Pitié-Salpêtrière, Department of Neuroradiology, Paris, F-75013, France.

[4] AP-HP, Hôpital Saint Antoine, Department of Radiology, Paris, F-75013, France.

[5] Sorbonne Universités, UPMC Univ Paris 06, Inserm, CNRS, Institut du cerveau et la moelle (ICM) - Hôpital Pitié-Salpêtrière, Paris, F-75013, France.

[6] Limoges University, Limoges, France

[7] INSERM U1171, National reference center for young onset dementia, Neurology department, University Hospital, Lille, France

[8] Lille University, Lille, France

[9] AP-HP, Hôpital Pitié-Salpêtrière, Department of Nuclear Medicine, Paris, F-75013, France.

[10] Laboratoire d'Imagerie Biomédicale, Sorbonne Universités, UPMC Univ Paris 06, Inserm U 1146, CNRS UMR 7371, Paris, France

[11] CNR-MAJ / Rouen University Hospital, INSERM 1245, Rouen, France

[12] Rouen University Hospital, Department of Neurology, F-76000, Rouen, France

[13] Division of Neurology V and Neuropathology, Fondazione IRCCS Istituto Neurologico Carlo Besta, Milano, Italy.

[14] AP-HP, Hôpital Pitié-Salpêtrière, Institute of Memory and Alzheimer's Disease (IM2A), Centre of excellence of neurodegenerative disease (CoEN), Department of Neurology, F-75013, Paris, France

[15] AP-HP, Hôpital Pitié-Salpêtrière, Centre de Référence des Démences Rares ou Précoces, Paris, F-75013, France.

[16] Centre pour l'Acquisition et le Traitement des Images (CATI), ICM, France.

* These authors contributed equally to the manuscript

Corresponding author:

Isabelle Le Ber

Institut du Cerveau et la Moelle (ICM) ; Hôpital Pitié-Salpêtrière; 47-83, boulevard de l'Hôpital, 75651 Paris Cedex 13, France.

Telephone: 0033 1 5727 4682

Fax: 0033 1 5727 4795

E-mail: isabelle.leber@upmc.fr

***The PrevDemAls study group includes:**

Eve Benchetrit (Hôpital Pitié-Salpêtrière, Paris), Hugo Bertin (Hôpital de la Salpêtrière, Paris), Anne Bertrand (Hôpital Pitié-Salpêtrière, Paris), Anne Bissery (Hôpital Pitié-Salpêtrière, Paris), Stéphanie Bombois (CHU Roger Salengro, Lille), Marie-Paule Boncoeur (CHU Limoges), Pascaline Cassagnaud (CHU Roger Salengro, Lille), Mathieu Chastan (CHU Charles Nicolle, Rouen), Yaohua Chen (CHU Roger Salengro, Lille), Marie Chupin (CATI, ICM, Paris), Olivier Colliot (ICM, Paris), Philippe Couratier (CHU Limoges), Xavier Delbeucq (CHU Roger Salengro, Lille), Vincent Deramecourt (CHU Roger Salengro, Lille), Christine Delmaire (CHU Roger Salengro, Lille), Emmanuel Gerardin (CHU Charles Nicolle, Rouen), Claude Hossein-Foucher (CHU Roger Salengro, Lille), Bruno Dubois (Hôpital Pitié-Salpêtrière, Paris), Marie-Odile Habert (Hôpital Pitié-Salpêtrière, Paris), Didier Hannequin (CHU Charles Nicolle, Rouen), Géraldine Lautrette (CHU Limoges), Thibaud Lebouvier (CHU Roger Salengro, Lille), Isabelle Le Ber (Hôpital Pitié-Salpêtrière Salpêtrière, Paris), Stéphane Lehéricy (Hôpital Pitié-Salpêtrière Salpêtrière, Paris), Benjamin Le Toullec (ICM, Paris), Richard Levy (Hôpital Pitié-Salpêtrière Salpêtrière, Paris), Olivier Martinaud (CHU Charles Nicolle, Rouen), Kelly Martineau (CATI, ICM, Paris), Marie-Anne Mackowiak (CHU Roger Salengro, Lille), Jacques Monteil (CHU Limoges), Florence Pasquier (CHU Roger Salengro, Lille), Grégory Petyt (CHU Roger Salengro, Lille), Pierre-François Pradat (Hôpital Pitié-Salpêtrière, Paris), Assi-Hervé Oya (Hôpital Pitié-Salpêtrière, Paris), Daisy Rinaldi (Hôpital Pitié-Salpêtrière, Paris), Adeline Rollin-Sillaire (CHU Roger Salengro, Lille), François Salachas (Hôpital Pitié-Salpêtrière, Paris), Sabrina Sayah (Hôpital Pitié-Salpêtrière, Paris), David Wallon (CHU Rouen).

Search Terms: Frontotemporal dementia (29); Amyotrophic Lateral Sclerosis (178); All Genetics (91); MRI (120); DWI (128)

Date of the revision: September 6th 2017

Word count: 3000

Tweet (117 characters) **Praxis impairment, atrophy & white matter alterations in *c9orf72* carriers ≤ 40 years of age**

Key points (75-100 words)

Question: How early can we detect changes in presymptomatic carriers of *c9orf72* mutation?

Findings: Praxis impairment, cortico-subcortical atrophy and white matter alterations can be detected in young *c9orf72* carriers, before 40 years of age.

Meaning: Early praxis impairment is an unexpected finding, which may reflect developmental abnormalities in presymptomatic *c9orf72* carriers. Cortico-subcortical atrophy appears diffuse, while white matter changes predominate in frontal white matter and corticospinal tracts, thus being more reflective of the expected phenotype of FTLD-ALS.

Abstract (350 words)

Importance: Presymptomatic carriers of *c9orf72* mutation, the most frequent genetic cause of FLTD and ALS, represent the optimal target population for the development of disease-modifying drugs. Preclinical biomarkers are needed in order to monitor the effect of therapeutic interventions in this population.

Objectives: To assess the occurrence of cognitive, structural and microstructural changes in presymptomatic *c9orf72* carriers.

Design, Setting & Participants: The PREVDEMALS study is a prospective, multicentric, observational study of first degree relatives of patients carrying *c9orf72* mutation. Eighty-four subjects entered the study between October 2015 and April 2017; 80 were included in cross-sectional analyses of baseline data. All subjects underwent neuropsychological testing and Magnetic Resonance Imaging (MRI); 63 underwent Diffusion Tensor MRI (DTI). Grey matter volumes and DTI metrics were calculated within regions of interest (ROI). Anatomical and microstructural differences between carriers (c9+) and non-carriers (c9-) were assessed using linear mixed-effects models.

Exposure: none

Main outcome and measure: Differences in neuropsychological scores, grey matter volume and white matter integrity between c9+ and c9-.

Results: There was 41 c9+ (mean age = 45.2 years ± 13.9; 24 females) and 39 c9- (mean age = 39.8 years ± 11.1; 24 females). Compared to c9-, c9+ had lower praxis score (163.4 ± 6.1 vs. 165.3 ± 5.9; p=.01) and intransitive gesture score (34.9 ± 1.6 vs. 35.7 ± 1.5; p=.004); atrophy in 8 cortical ROI and in the right thalamus; white matter alterations in 8 tracts. When restricting the analyses to subjects before 40 years of age, c9+ had lower praxis score and intransitive gesture score; atrophy in 4 cortical ROI and in the right thalamus; white matter alterations in 2 tracts.

Conclusions and Relevance: Cognitive, anatomical and microstructural alterations are detectable in young *c9orf72* mutation carriers. Early and subtle praxis alterations, underpinned by focal atrophy of the left supramarginal gyrus, may represent an early and non-evolving phenotype related to neurodevelopmental effects of *c9orf72* mutation. White matter alterations reflect the future phenotype of FTLD/ALS, while atrophy appears more diffuse. Our results contribute to a better understanding of the preclinical phase of *c9orf72* disease, and of the respective contribution of MR biomarkers.

Introduction

Frontotemporal lobar degeneration (FTLD) and amyotrophic lateral sclerosis (ALS) are neurodegenerative diseases with common genetic causes, the most frequent being a GGGGCC repeat expansion in *c9orf72* gene[1,2]. This expansion may lead to a loss of *c9orf72* function, and causes abnormal neuronal aggregation of nuclear RNA foci, dipeptides repeats (DPR) and TDP-43 inclusions[3]. Recent preclinical development of disease-modifying drugs, such as antisense oligonucleotides that target mutant RNA, offer promising therapeutic perspectives in *c9orf72* disease[4,5].

Presymptomatic carriers of genetic mutation represent the optimal target population for the development of new disease-modifying treatments against FTLD and ALS. It is now established that neurodegenerative diseases cause biological and morphological changes decades before symptom onset[6]; thus, the presymptomatic stage represents the best time-window for therapeutic interventions, by allowing the possibility to stop the neurodegenerative process before irreversible brain damage. Establishing the chronology of structural and microstructural changes during the presymptomatic stage is thus crucial, in order to identify markers of disease progression and monitor the effect of treatments. Three studies have suggested that atrophy, studied with anatomical MRI, could be detected years before symptom onset in *c9orf72* presymptomatic carriers[7–9], but were limited by the small number of participants. One study also detected alterations of white matter integrity, using diffusion MRI[9], but another failed to identify such changes[8]. The present work aims at assessing cognitive, structural and microstructural changes in a large cohort of asymptomatic *c9orf72* carriers, in order to characterize the presymptomatic course of the disease and identify potential neuroimaging biomarkers of preclinical disease progression.

Material and Methods

Participants

Eighty-four individuals out of 48 *c9orf72* families, all first degree relatives of *c9orf72* mutation carriers, were enrolled in a national multicentric study (PrevDemAls) between 2015 and 2017.

At inclusion, asymptomatic status of participants was ascertained based on relative's interview, neurological examination and the normality of behavioral scales and neuropsychological scores, taking into account age and educational level. Neuropsychological tests are detailed in eMethod1. Two participants were excluded from the analysis because mild cerebellar syndrome or cognitive impairment were detected during the visit; two other participants were excluded because of incomplete MRI protocol. Eighty neurologically healthy participants were finally included in the analyses. The *c9orf72* genetic status was determined by repeat-primed-PCR on lymphocytes DNA. Forty-one participants (c9+) carried a pathogenic expansion (>23 GGGGCC repeats); 39 participants without expansion (c9-) constituted the control group. Expected ages at onset of *c9orf72* carriers were estimated by averaging the ages at onset of affected relatives, similarly to previous studies[7].

Standard Protocol Approvals, Registrations, and Patient Consents

This study was approved by the local ethical committee; written informed consent was obtained from all participants.

MRI acquisition

All MRI acquisitions were performed on a 3T MR system (Siemens Prisma 3T n= 64; Philips Achieva 3T n= 9; GE 3T n=7), in 3 imaging centers belonging to the harmonized national

network of CATI (Centre d'Acquisition et de Traitement d'Images, cati-neuroimaging.com/)[10]. CATI performs on-site visits for the setup of imaging protocols and regular follow-up. 3DT1 sequence parameters were similar for the 3 centers, while DTI sequence was performed in only one center (see eMethod2 for detailed sequence parameter). Systematic quality check of MR images were performed by CATI, using a dedicated software programme with quantitative and qualitative indices, allowing the check for 1) protocol consistency (MRI scanner, software version, type of reception coil, acquisition slab position, sequence parameters and sequence order); 2) presence and localization of artifacts (motion artifacts, spike artifacts, other); 3) overall image quality based on signal-to-noise ratio, contrast-to-noise ratio and intensity non-uniformity[10]. Among the 80 MR dataset, 75 (94%) were considered of good quality and 5 (6%) of acceptable quality.

Anatomical MRI processing

FreeSurfer image analysis software 5.3 (http://surfer. nmr.mgh.harvard.edu) was used to process the T1-weighted images. The processing pipeline included non-uniformity and intensity correction, skull stripping, grey/white matter segmentation, reconstruction of the cortical surface, extraction of cortical ROI volumes using the Desikan atlas, and subcortical ROI volumes and total intracranial volume (TIV) using the aseg atlas. We used for analyses the normalized volume of each ROI, defined as NVROI = (TIVm.VROI)/TIV, where TIVm is the average total intracranial volume computed across all participants, which is constant, and VROI is the volume of the ROI. The role of the constant multiplicative factor TIVm is simply to preserve the order of magnitude of NVROI similar to that of VROI.

Diffusion MRI processing

All raw DWI volumes were aligned to the average b0 image with first 6 degrees of freedom (dof), to correct for head motion, and diffusion directions were appropriately updated[11]. A registration with 12 dof was used to correct for eddy current distortions. These registrations were done using the FSL flirt tool (www.fmrib.ox.ac.uk/fsl). Field map image was used to correct for echo-planar imaging (EPI) induced susceptibility artifacts[12] with the FSL prelude/fugue tools. DWI volumes were corrected for nonuniform intensity using ANTs N4 bias correction algorithm[13]. A single multiplicative bias field from the averaged b0 image was estimated[14]. The DWI datasets were up-sampled at 1mm in order to improve the registration between the T1-weighted image and the DWI. A diffusion tensor model was fitted at each voxel to calculate Fractional Anisotropy (FA), Mean Diffusivity (MD), Radial Diffusivity (RD) and Axial Diffusivity (AD) maps. White matter tracts were defined using the JHU white-matter tractography atlas[15], with a 25% probabilistic threshold. For each subject, the FA map was registered onto the JHU atlas template with the ANTs SyN algorithm[16]. Then, the estimated non-linear deformation was applied to the parametric maps and we extracted, in each patient, the average values of DTI metrics (FA, MD, RD and AD) within each tract of the JHU atlas.

Statistical analysis

Statistical analyses were performed using R 3.4.0 (The R Foundation for Statistical Computing, Vienna, Austria) and GraphPad Prism 7.0 (La Jolla, CA, USA). Demographic characteristics and clinical tests were compared between groups using chi-squared test (for dichotomous and categorical variables) or Mann-Whitney test (for numerical variables). Structural and microstructural differences between carriers and non-carriers of the *c9orf72* mutation were assessed using linear mixed-effects models. We used real age and group (i.e.,

mutation status) as fixed effects, and family membership as random effect, with the following model:

$$Y_{ik}{}^{(j)} = \mu + \beta \times gender_i + \lambda \times age_i + \eta \times group_i + \mathrm{U}_k + \epsilon_{ik}{}^{(j)}$$

where $Y_{ik}{}^{(j)}$ is the response of the j^{th}region of interest (ROI) for the i^{th} subject and the k^{th} family; $gender_i$, age_i and $group_i$ are the fixed effects; μ, β, λ and η are their estimated parameters; U_k is the random effect measuring the difference between the average response in the family and in the whole population; $\epsilon_{ik}{}^{(j)}$ is the random error.

Correlation between real age and expected years to onset was assessed using Pearson correlation coefficient. Correlations between clinical scores and structural or microstructural measures in presymptomatic carriers were assessed using Spearman correlation coefficient.

Statistical significance was set at $p < 0.05$. Corrections for multiple comparisons were performed using Benjamini-Hochberg method. All statistical analyses were performed independently by two scientists (J.W. & M.H.).

Results

Participants

There were no statistical differences between c9+ and c9- subjects regarding age at evaluation and demographic characteristics (Table 1). In c9+ subjects, real age and expected years to onset were strongly correlated (eFigure 1, $p < .001$; $r^2 = 0.802$, Pearson correlation coefficient), with a mean estimated age of onset of 58.9 ± 4.9 years. C9+ subjects had significantly lower praxis score; this difference remained statistically significant in subjects ≤ 40-year-old, who were 25.4 ± 8.1 years to onset (165.2 ± 3.4 in c9+ vs. 167.6 ± 0.6 in c9-, p=.036). Praxis score was significantly correlated with age in both c9+ and c9- (Fig. 1B). When analyzing the subscores of praxis test, all were lower for the c9+ group, but statistical significance was reached only for the subscore of non-transitive gestures (Fig. 1C); this

difference remained statistically significant in subjects ≤ 40-year-old (35.0 ± 1.7 in c9+ vs. 36 ± 0 in c9-, p = .036). Lastly, the total recall score of the FCRT test was significantly lower in c9+ as compared to c9- (Fig. 1E), but with a large overlap of scores between the 2 groups (Fig. 1F), and no significant difference among subjects ≤ 40-year-old (47 ± 1.3 in c9+ vs. 47 ± 1.4 in c9-, p = .08).

Effect of c9orf72 mutation on cortical structures

C9+ subjects showed diffuse cortical atrophy within the associative cortex, with a sparring of primary sensorimotor and visual cortex, frontobasal cortex and superior temporal cortex (Fig. 2A). After correction for multiple comparisons, this effect remained significant for one frontal, three inferior temporal and four parietal ROI (Fig.2B and eTable 1). In these 8 ROI, we performed the same analyses restricted to the subjects ≤ 40 years of age, and found significant atrophy within right caudal middle frontal cortex, left and right precuneus and left supramarginal cortex.

Effect of c9orf72 mutation on subcortical structures

C9+ subjects showed significant atrophy in left and right thalamus, as compared to c9- subjects (Fig.2A). After correction for multiple comparisons, effect remained significant for the right thalamus (Fig.2B and eTable 2), and persisted when restricting the analysis to the subjects ≤ 40 years of age.

Effect of c9orf72 mutation on white matter microstructure

C9+ subjects showed diffuse alteration of white matter microstructure (decreased FA, increased MD, AD and RD), predominating in frontal regions and affecting corticospinal tracts, bilaterally (Fig.4, eTable 3 and eFigure2). Only for this modality, we observed that the

oldest c9+ subject was an outlier for some DTI metrics (eFigure2); to make sure that results were not driven by this outlier, we performed the same analyses without it, and still found significant differences in 23 DTI metrics (instead of 27), within the same white matter tracts. After correction for multiple comparisons, eight tracts remained significantly altered: the left corticospinal tract, the right anterior thalamic radiation, four tracts connected to the frontal lobes (forceps minor, bilateral inferior fronto-occipital fasciculus and right superior longitudinal fasciculus) and two tracts connected to the temporal lobes (bilateral inferior longitudinal fasciculus). In these tracts, we performed the same analyses restricted to the subjects ≤ 40 years of age, and still found significant increased RD and decreased FA within the right anterior thalamic radiation, and increased RD within the right forceps minor.

Correlation between structural changes and clinical scores

We looked for possible correlations between the neuropsychological scores altered in c9+ subjects (praxis, intransitive gestures and FCRT scores), and the markers of structural and microstructural alterations in c9+ subjects (volume of cortical and subcortical regions and DTI metrics significantly altered in c9+, after correction for multiple comparisons). No correlation was found between the 3 scores and structural or microstructural changes.

Discussion

The present work, in a large cohort of presymptomatic *c9orf72* carriers, reveals unexpected results. We show that cognitive, structural and microstructural changes can be detected very early in c9+ subjects, from 20 to 40 years of age, corresponding to 25.4 ± 8.1 years to expected onset. We also show that praxis appears as the first cognitive domain to be altered in young c9+. Lastly, we show that presymptomatic c9+ subjects display distinct patterns of

atrophy and white matter alterations: cortico-subcortical atrophy appears as a diffuse process, while white matter microstructural changes predominate in the areas specifically affected during FTLD-ALS.

In this study, we choose to model the effect of *c9orf72* mutation on atrophy and white matter microstructure using the real age of subjects. Instead of real age, some authors[7] have used the distance to mean age of onset in affected relatives, as an estimation of expected years to onset in presymptomatic carriers of *c9orf72*. However, age of onset is highly variable even within individuals of the same family, one of the possible reasons being a possible anticipation phenomenon[17]. Thus, it must be highlighted that quantification of the effects of *c9orf72* mutation on brain structure remains currently limited by the difficulty to accurately estimate expected age at onset in presymptomatic carriers.

Cognitive, structural and microstructural changes are detected in young c9+ subjects

During the preclinical course of neurodegenerative diseases, structural changes are expected 10-15 years and clinical changes 5 years before expected symptom onset, according to the largest presymptomatic FTLD[7] and Alzheimer's disease cohorts[18,19]. However, the pace of progression varies depending on the underlying mutation. In *c9orf72*-FTLD patients, disease duration can be remarkably long[20–22] and atrophy progresses at a slow rate[23], as compared to other genetic or sporadic forms. Thus, it is conceivable that the preclinical phase of *c9orf72* disease would last particularly long. Our study evidences that subtle cognitive, structural and microstructural alterations can be detected in young *c9orf72* carriers before 40 years of age. This finding suggests that young subjects may represent the optimal target population for future disease-modifying interventions. Previous studies have suggested that atrophy emerge in young *c9orf72* carriers[7,9], either based on group differences obtained on extrapolated measures[7], or because no acceleration of atrophy was detected during aging in *c9orf72*

carriers[9]. Our results confirm this hypothesis, by showing significant differences of metrics directly measured in young c9+ and c9- subjects.

Praxis impairment is an early feature of c9orf72 disease

The evidence of subtle praxis alterations in young c9+ subjects is a surprising result. One study has suggested that cognitive and behavioral changes could occur 10 to 15 years from symptom onset in presymptomatic *c9orf72* carriers, based on extrapolated data[7]; however, praxis evaluation was not reported. Our result is particularly striking, as a clear separation was visible between the praxis scores of c9+ and c9- young individuals (Fig. 1B). Praxis score has been reported to decrease during normal aging[24,25]; similarly, it was inversely correlated with age in both c9- and c9+ subjects in our study (Fig1B). The difficulty of this task may explain its sensitivity to detect subtle preclinical changes in c9+ subjects. The observed impairment in non-transitive gestures (symbolic gestures without the use of an object) is a feature of ideomotor apraxia, which involves the posterior part of the left parietal lobe, mainly the left supramarginal gyrus[26]. Consistently, the impairment in non-transitive gestures in young c9+ subjects was associated with a focal atrophy of this region (i.e., left supramarginal cortex). No correlation was detected between volume of left supramarginal cortex and non-transitive gesture score in c9+ subjects; this lack of correlation was likely related to the relatively low variance of the score, which was only slightly altered in c9+ (1 to 6 points below the normal score of 36, see Fig.1D). Praxis alteration was unexpected, as it is not a salient feature of *c9orf72* FTLD; although it has been occasionally reported[27–30], it is usually less marked than executive and behavioral dysfunction[31–34]. Thus, praxis impairment may represent an early-expressed and non-evolving phenotype of *c9orf72* mutation. These intriguing findings stress the need to characterize *c9orf72* mutation alterations on the scale of the entire lifespan of mutation carriers, including childhood, in order to disentangle possible

developmental alterations[8,9], from potential preclinical prognostic markers of *c9orf72* disease. It also emphasizes the fact that neuropsychological features of *c9orf72* mutation may extend well beyond the classical spectrum of FTLD, and require extensive neuropsychological characterization.

Additionally, we also observed a slight decrease in recall performance in c9+ carriers. Interestingly, *c9orf72* mutation is associated with abnormal deposition of TDP-43, DPR and RNA foci in the hippocampus[35]. However, the slight memory impairment we observed appeared less striking than praxis impairment: there was a large overlap of values between c9+ and c9- subjects, and the difference did not persist when restricting the analysis to subjects ≤ 40 years of age. Moreover, we did not detect any significant atrophy in the hippocampus of c9+ subjects.

C9orf72 mutation is associated with early thalamic atrophy

Thalamic atrophy appears as a reliable effect of *c9orf72* mutation. Thalamic atrophy has been previously reported in smaller cohorts of presymptomatic *c9orf72* carriers[7–9], and also in symptomatic *c9orf72* carriers with FTLD[33,37,38] or ALS[39]. Thalamic atrophy may be related to the presence of pathological deposits, i.e. TDP-43 and/or DPR, but it can also be caused by deafferentation processes secondary to the diffuse cortical atrophy, due to the high number of connections between the hemispheric cortex and the thalamus. These mechanisms are not exclusive and may be associated, which would explain the high sensitivity of previous studies for detecting early thalamic atrophy in c9+ subjects.

White matter microstructural changes, but not cortical atrophy, reflects the expected topography of FTLD-ALS in c9+ subjects

Our study demonstrates a major difference of pattern between atrophy and white matter alterations in c9+ subjects. Atrophy appears as a widespread phenomenon, with a relative sparing of primary motor cortex and frontobasal cortex, areas that are preferentially involved during ALS and FTLD, respectively (Fig. 3). Conversely, white matter alterations seem to preferentially target corticospinal tracts and frontal white matter (Fig. 4). These suggest that in c9+ subjects, white matter changes may be more predictive of future cognitive and motor deficits than cortical atrophy. These different patterns are reminiscent of the topography of the two histopathological hallmarks of *c9orf72* mutation, DPR and TDP-43. Even if this is still debated, DPR deposits have a diffuse distribution unrelated to the clinical phenotype of patients[40–43], and seem to precede TDP-43 deposition[44]. Conversely, TDP-43 deposits may represent a downstream process more correlated to clinical symptoms. Furthermore, TDP-43 deposits are present both in cortical neurons and white matter glial cells[45]; thus, white matter changes, possibly more reflective of future clinical deficits, may relate more to TDP-43 pathology than to DPR in presymptomatic *c9orf72* disease.

Conclusion

The present work demonstrates that pathological processes emerge during early adulthood in *c9orf72* mutation carriers. Early and subtle praxis alterations in young c9+ subjects, underpinned by a focal atrophy of the left supramarginal gyrus, may represent a non-evolving phenotype, which highlights the possible overlaps and intricacy between neurodevelopmental and neurodegenerative processes. The distinct patterns of atrophy and white matter changes observed in c9+ subjects suggest that white matter integrity might be more reflective of the future FTLD/ALS phenotype than atrophy. Our results contribute to a better understanding of

the spectrum of *c9orf72* disease, and of the respective contribution of MR biomarkers in assessing disease-related changes.

Acknowledgements

This study was funded by Assistance Publique – Hôpitaux de Paris (Clinical Research and Development Department), grant ANR/DGOS PRTS 2015-2019 PrevDemAls (to I.L.B.) and by "Investissements d'avenir" ANR-10-IAIHU-06 (Agence Nationale de la Recherche-10-Investissements-Avenir-Institut-Hospitalo-Universitaire-06). O.C. is supported by a "Contrat d'Interface Local" from Assistance Publique-Hôpitaux de Paris (AP-HP). The study was conducted with the support of the Centre d'Investigation Clinique (CIC 1422), and the Centre pour l'Acquisition et le Traitement des Images (CATI) platform, at IHU-A-ICM, Paris, France.

This study has been registered on the website http://clinicaltrials.gov/ under number NCT02590276.

The funding sources had no role in design and conduct of the study; collection, management, analysis, and interpretation of the data; preparation, review, or approval of the manuscript; and decision to submit the manuscript for publication.

Competing financial interests related to the present article: none to disclose for all authors.

Competing financial interests unrelated to the present article: BD received consultant fees from Eli Lilly, Cytox Ltd, and Boehringer Ingelheim, and he received funding for his institution from Merck, Pfizer and Roche. OC and SD are funded by European Union's

Horizon 2020 research and innovation programme under grant agreement No 666992 (EuroPOND), and No. 720270 (HBP SGA1). SD is funded by European Research Council (ERC) under grant agreement No 678304. M-OH reported payments for lectures from Piramal and Eli Lilly. PC received consultant fees from Boehringer Ingelheim and funding for his institution from Cytokinetics

Anne Bertrand and Junhao Wen had full access to all the data in the study and takes responsibility for the integrity of the data and the accuracy of the data analysis.

Authors' contribution:

Anne Bertrand: Study concept, statistical analyses, interpretation of the results, writing the first version of the manuscript.

Junhao Wen: Study concept, data acquisition and statistical analyses, interpretation of the results, revising the manuscript.

Daisy Rinaldi: data acquisition, interpretation of the results, revising the manuscript.

Marion Houot: statistical analyses, interpretation of the results, revising the manuscript.

Sabrina Sayah: data acquisition, interpretation of the results, revising the manuscript.

Agnès Camuzat: data acquisition, interpretation of the results, revising the manuscript.

Clémence Fournier: data acquisition, interpretation of the results, revising the manuscript.

Sabrina Fontanella: data acquisition, revising the manuscript.

Alexandre Routier: data acquisition, revising the manuscript.

Philippe Couratier: data acquisition, revising the manuscript.

Florence Pasquier: data acquisition, revising the manuscript.

Marie-Odile Habert: data acquisition, revising the manuscript.

Didier Hannequin: data acquisition, revising the manuscript.

Olivier Martinaud: data acquisition, revising the manuscript.

Paola Caroppo: data acquisition, interpretation of the results, revising the manuscript.

Richard Levy: Study concept, interpretation of the results, revising the manuscript.

Bruno Dubois: Study concept, interpretation of the results, revising the manuscript.

Alexis Brice: Study concept, interpretation of the results, revising the manuscript.

Stanley Durrleman: Study concept, interpretation of the results, revising the manuscript.

Olivier Colliot: Study concept, interpretation of the results, revising the manuscript.

Isabelle le Ber: Study concept, data acquisition, interpretation of the results, writing the final version of the manuscript.

References

1. DeJesus-Hernandez M, Mackenzie IR, Boeve BF, et al. Expanded GGGGCC hexanucleotide repeat in noncoding region of C9ORF72 causes chromosome 9p-linked FTD and ALS. *Neuron*. 2011;72(2):245-256. doi:10.1016/j.neuron.2011.09.011.

2. Renton AE, Majounie E, Waite A, et al. A hexanucleotide repeat expansion in C9ORF72 is the cause of chromosome 9p21-linked ALS-FTD. *Neuron*. 2011;72(2):257-268. doi:10.1016/j.neuron.2011.09.010.

3. Cruts M, Gijselinck I, Van Langenhove T, van der Zee J, Van Broeckhoven C. Current insights into the C9orf72 repeat expansion diseases of the FTLD/ALS spectrum. *Trends Neurosci*. 2013;36(8):450-459. doi:10.1016/j.tins.2013.04.010.

4. Donnelly CJ, Zhang P-W, Pham JT, et al. RNA toxicity from the ALS/FTD C9ORF72 expansion is mitigated by antisense intervention. *Neuron*. 2013;80(2):415-428. doi:10.1016/j.neuron.2013.10.015.

5. Jiang J, Zhu Q, Gendron TF, et al. Gain of Toxicity from ALS/FTD-Linked Repeat Expansions in C9ORF72 Is Alleviated by Antisense Oligonucleotides Targeting GGGGCC-Containing RNAs. *Neuron*. 2016;90(3):535-550. doi:10.1016/j.neuron.2016.04.006.

6. Bateman RJ, Xiong C, Benzinger TLS, et al. Clinical and biomarker changes in dominantly inherited Alzheimer's disease. *N Engl J Med*. 2012;367(9):795-804. doi:10.1056/NEJMoa1202753.

7. Rohrer JD, Nicholas JM, Cash DM, et al. Presymptomatic cognitive and neuroanatomical changes in genetic frontotemporal dementia in the Genetic Frontotemporal dementia Initiative (GENFI) study: a cross-sectional analysis. *Lancet Neurol*. 2015;14(3):253–262.

8. Walhout R, Schmidt R, Westeneng H-J, et al. Brain morphologic changes in asymptomatic C9orf72 repeat expansion carriers. *Neurology*. 2015;85(20):1780–1788.

9. Lee SE, Sias AC, Mandelli ML, et al. Network degeneration and dysfunction in presymptomatic C9ORF72 expansion carriers. *NeuroImage Clin*. December 2016. doi:10.1016/j.nicl.2016.12.006.

10. Operto G, Chupin M, Batrancourt B, et al. CATI: A Large Distributed Infrastructure for the Neuroimaging of Cohorts. *Neuroinformatics*. 2016;14(3):253-264. doi:10.1007/s12021-016-9295-8.

11. Leemans A, Jones DK. The B-matrix must be rotated when correcting for subject motion in DTI data. *Magn Reson Med*. 2009;61(6):1336-1349. doi:10.1002/mrm.21890.

12. Jezzard P, Balaban RS. Correction for geometric distortion in echo planar images from B0 field variations. *Magn Reson Med*. 1995;34(1):65-73.

13. Tustison NJ, Avants BB. Explicit B-spline regularization in diffeomorphic image registration. *Front Neuroinformatics*. 2013;7:39. doi:10.3389/fninf.2013.00039.

14. Jeurissen B, Tournier J-D, Dhollander T, Connelly A, Sijbers J. Multi-tissue constrained spherical deconvolution for improved analysis of multi-shell diffusion MRI data. *NeuroImage*. 2014;103:411-426. doi:10.1016/j.neuroimage.2014.07.061.

15. Mori S, Wakana S, Nagae-Poetscher L, van Zijl P. *MRI Atlas of Human White Matter*. Amsterdam: Elsevier; 2005.

16. Avants BB, Epstein CL, Grossman M, Gee JC. Symmetric diffeomorphic image registration with cross-correlation: evaluating automated labeling of elderly and neurodegenerative brain. *Med Image Anal*. 2008;12(1):26-41. doi:10.1016/j.media.2007.06.004.

17. Bateman RJ, Xiong C, Benzinger TLS, et al. Clinical and Biomarker Changes in Dominantly Inherited Alzheimer's Disease. *N Engl J Med*. 2012;367(9):795-804. doi:10.1056/NEJMoa1202753.

18. Benzinger TLS, Blazey T, Jack CR, et al. Regional variability of imaging biomarkers

in autosomal dominant Alzheimer's disease. *Proc Natl Acad Sci U S A*. 2013;110(47):E4502-4509. doi:10.1073/pnas.1317918110.

19. Gómez-Tortosa E, Gallego J, Guerrero-López R, et al. C9ORF72 hexanucleotide expansions of 20-22 repeats are associated with frontotemporal deterioration. *Neurology*. 2013;80(4):366-370. doi:10.1212/WNL.0b013e31827f08ea.

20. Khan BK, Yokoyama JS, Takada LT, et al. Atypical, slowly progressive behavioural variant frontotemporal dementia associated with C9ORF72 hexanucleotide expansion. *J Neurol Neurosurg Psychiatry*. 2012;83(4):358-364. doi:10.1136/jnnp-2011-301883.

21. Suhonen N-M, Kaivorinne A-L, Moilanen V, et al. Slowly progressive frontotemporal lobar degeneration caused by the C9ORF72 repeat expansion: a 20-year follow-up study. *Neurocase*. 2015;21(1):85-89. doi:10.1080/13554794.2013.873057.

22. Whitwell JL, Boeve BF, Weigand SD, et al. Brain atrophy over time in genetic and sporadic frontotemporal dementia: a study of 198 serial magnetic resonance images. *Eur J Neurol*. 2015;22(5):745-752. doi:10.1111/ene.12675.

23. Peigneux P, van der Linden M. Influence of ageing and educational level on the prevalence of body-part-as-objects in normal subjects. *J Clin Exp Neuropsychol*. 1999;21(4):547-552. doi:10.1076/jcen.21.4.547.881.

24. Rodrigues Cavalcante K, Caramelli P. Evaluation of the performance of normal elderly in a limb praxis protocol: influence of age, gender, and education. *J Int Neuropsychol Soc JINS*. 2009;15(4):618-622. doi:10.1017/S1355617709090663.

25. Króliczak G, Piper BJ, Frey SH. Specialization of the left supramarginal gyrus for hand-independent praxis representation is not related to hand dominance. *Neuropsychologia*. 2016;93(Pt B):501-512. doi:10.1016/j.neuropsychologia.2016.03.023.

26. Floris G, Borghero G, Cannas A, et al. Constructional apraxia in frontotemporal dementia associated with the C9orf72 mutation: broadening the clinical and

neuropsychological phenotype. *Amyotroph Lateral Scler Front Degener*. 2015;16(1-2):8-15. doi:10.3109/21678421.2014.959450.

27. Mahoney CJ, Beck J, Rohrer JD, et al. Frontotemporal dementia with the C9ORF72 hexanucleotide repeat expansion: clinical, neuroanatomical and neuropathological features. *Brain*. 2012;135(3):736-750. doi:10.1093/brain/awr361.

28. Mahoney CJ, Downey LE, Ridgway GR, et al. Longitudinal neuroimaging and neuropsychological profiles of frontotemporal dementia with C9ORF72 expansions. *Alzheimers Res Ther*. 2012;4(5):41.

29. Van Langenhove T, van der Zee J, Gijselinck I, et al. Distinct clinical characteristics of C9orf72 expansion carriers compared with GRN, MAPT, and nonmutation carriers in a Flanders-Belgian FTLD cohort. *JAMA Neurol*. 2013;70(3):365-373. doi:10.1001/2013.jamaneurol.181.

30. Devenney E, Hornberger M, Irish M, et al. Frontotemporal Dementia Associated With the *C9ORF72* Mutation: A Unique Clinical Profile. *JAMA Neurol*. 2014;71(3):331. doi:10.1001/jamaneurol.2013.6002.

31. Floeter MK, Traynor BJ, Farren J, et al. Disease progression in *C9orf72* mutation carriers. *Neurology*. June 2017:10.1212/WNL.0000000000004115. doi:10.1212/WNL.0000000000004115.

32. Sha SJ, Takada LT, Rankin KP, et al. Frontotemporal dementia due to C9ORF72 mutations: Clinical and imaging features. *Neurology*. 2012;79(10):1002. doi:10.1212/WNL.0b013e318268452e.

33. Suhonen N-M, Haanpää RM, Korhonen V, et al. Neuropsychological Profile in the C9ORF72 Associated Behavioral Variant Frontotemporal Dementia. *J Alzheimers Dis*. 2017;58(2):479-489. doi:10.3233/JAD-161142.

34. Mackenzie IRA, Frick P, Neumann M. The neuropathology associated with repeat

expansions in the C9ORF72 gene. *Acta Neuropathol (Berl)*. 2014;127(3):347-357. doi:10.1007/s00401-013-1232-4.

35. Floeter MK, Bageac D, Danielian LE, Braun LE, Traynor BJ, Kwan JY. Longitudinal imaging in C9orf72 mutation carriers: Relationship to phenotype. *NeuroImage Clin*. 2016;12:1035-1043. doi:10.1016/j.nicl.2016.10.014.

36. Mahoney CJ, Beck J, Rohrer JD, et al. Frontotemporal dementia with the C9ORF72 hexanucleotide repeat expansion: clinical, neuroanatomical and neuropathological features. *Brain*. 2012;135(3):736-750. doi:10.1093/brain/awr361.

37. Agosta F, Ferraro PM, Riva N, et al. Structural and functional brain signatures of C9orf72 in motor neuron disease. *Neurobiol Aging*. June 2017. doi:10.1016/j.neurobiolaging.2017.05.024.

38. Davidson Y, Robinson AC, Liu X, et al. Neurodegeneration in frontotemporal lobar degeneration and motor neurone disease associated with expansions in *C9orf72* is linked to TDP-43 pathology and not associated with aggregated forms of dipeptide repeat proteins. *Neuropathol Appl Neurobiol*. 2016;42(3):242-254. doi:10.1111/nan.12292.

39. Davidson YS, Barker H, Robinson AC, et al. Brain distribution of dipeptide repeat proteins in frontotemporal lobar degeneration and motor neurone disease associated with expansions in C9ORF72. *Acta Neuropathol Commun*. 2014;2:70. doi:10.1186/2051-5960-2-70.

40. Gomez-Deza J, Lee Y-B, Troakes C, et al. Dipeptide repeat protein inclusions are rare in the spinal cord and almost absent from motor neurons in C9ORF72 mutant amyotrophic lateral sclerosis and are unlikely to cause their degeneration. *Acta Neuropathol Commun*. 2015;3:38. doi:10.1186/s40478-015-0218-y.

41. Mackenzie IRA, Frick P, Grässer FA, et al. Quantitative analysis and clinico-pathological correlations of different dipeptide repeat protein pathologies in C9ORF72

mutation carriers. *Acta Neuropathol (Berl)*. 2015;130(6):845-861. doi:10.1007/s00401-015-1476-2.

42. Vatsavayai SC, Yoon SJ, Gardner RC, et al. Timing and significance of pathological features in *C9orf72* expansion-associated frontotemporal dementia. *Brain*. 2016;139(12):3202-3216. doi:10.1093/brain/aww250.

43. Neumann M, Kwong LK, Truax AC, et al. TDP-43-positive white matter pathology in frontotemporal lobar degeneration with ubiquitin-positive inclusions. *J Neuropathol Exp Neurol*. 2007;66(3):177-183. doi:10.1097/01.jnen.0000248554.45456.58.

44. Van Mossevelde S, van der Zee J, Gijselinck I, et al. Clinical Evidence of Disease Anticipation in Families Segregating a C9orf72 Repeat Expansion. *JAMA Neurol*. 2017;74(4):445-452. doi:10.1001/jamaneurol.2016.4847.

Figure legends

Fig. 1: Early cognitive changes in *c9orf72* mutation carriers. Compared to c9-, c9+ subjects showed significantly lower praxis scores (163.4 ± 6.1 vs. 165.3 ± 5.9, p = .011, Mann-Whitney test, 1A), significantly lower intransitive gesture subscore (34.9 ± 1.6 vs. 35.7 ± 1.5, p=.004, Mann-Whitney test, 1C), and significantly lower Free Cued and Recall score (46.4 ± 1.5 vs. 47.1 ± 1.5, p=.005, Mann-Whitney test, 1E). In both c9+ and c9- subjects, praxis score was significantly correlated with age (p = .013 and .001; r = - 0.387 and – 0.508, respectively, Spearman correlation coefficient; correlation assessed after removal of the 2 outliers with a score of 13). Other scores did not correlate with age. Box extend from 25th to 75th percentiles; whiskers from 5th to 95th percentile, and outliers are presented as scattered plots. The exact position of x-values (age) is not provided, in order to prevent individual subjects from identifying their mutation status.

Fig. 2: Cortical atrophy in *c9orf72* mutation carriers. Color-coded representation of p-values corresponding to the effect of *c9orf72* mutation on the volume of cortical ROI, before (A) and after (B) correction for multiple comparisons. Graphs of normalized cortical volumes as a function of age in c9- and c9+ subjects (C). The exact position of x-values (age) is not provided, in order to prevent individual subjects from identifying their mutation status.

Fig. 3: Subcortical atrophy in *c9orf72* mutation carriers. Color-coded representation of p-values corresponding to the effect of *c9orf72* mutation on the volume of subcortical structures, (A) before and (B) after correction for multiple comparisons. Graphs of normalized thalamic volumes as a function of age in c9- and c9+ subjects (C, D). The exact position of x-

values (age) is not provided, in order to prevent individual subjects from identifying their mutation status.

Fig. 4: Alterations of white matter in *c9orf72* mutation carriers. Color-coded representation of p-values corresponding to the effect of *c9orf72* mutation on the DTI scalars of white matter ROI, before (left side) and after (right side) correction for multiple correction.

Table 1. Study group characteristics. Values are expressed as mean ± standard deviation, or as number (%). N.A.: non-available. Significant p values are shown in bold. Minimum and maximum are not shown, in order to prevent individual subjects from identifying their mutation status. Next to each neuropsychological score is indicated, in brackets, the score obtained if all items of the test are correctly performed.

	c9-	c9+	p value
Total number	39	41	-
including subjects ≤ 40-year-old	16	22	-
Demographic characteristics			
Age (years)	45.2 ± 13.9	39.8 ± 11.1	.08
Female gender	24 (61.5%)	24 (58.5%)	.78
Laterality: right	33 (84.6%)	35 (85.4%)	.92
Familial phenotype: FLTD/ALS/mixed/N.A.	15/2/21/1	18/3/20/0	.77
Expected years to onset	-	-19.3 ± 11.2	-
Neuropsychological scores			
MMSE score (/30)	28.8 ± 1.5	28.6 ± 1.3	.34
MDRS score			
- Total score(/144)	141.5 ± 3.2	141.4 ± 2.6	.54
- Initiation (/37)	36.5 ± 1.3	36.6 ± 1.1	.72
- Concept (/39)	38.3 ± 1.2	38.3 ± 1.1	.75
- Attention (/37)	36.7 ± 0.8	36.7 ± 0.6	.95
- Construction (/6)	5.9 ± 0.2	6.0 ± 0.0	.23
- Memory (/25)	24.0 ± 1.4	23.8 ± 1.6	.81
FBI (0)	0.8 ± 1.8	1.3 ± 2.6	.54
FAB score (/18)	16.8 ± 1.4	17.1 ± 0.9	.39
Mini-SEA			
- Emotion recognition test (/35)	29.9 ± 2.7	29.8 ± 2.5	.73
- Faux-pas test (/30)	26.2 ± 4.7	25.6 ± 3.5	.13
Praxis score			
- Total score (/168)	165.3 ± 5.9	163.4 ± 6.1	**.01**
- Finger dexterity (/36)	35.5 ± 1.2	35.4 ± 1.2	.57
- Melokinetic apraxia (/24)	23.2 ± 1.5	22.8 ± 2.3	.37
- Non-representational gestures (/36)	35.7 ± 0.9	35.4 ± 1.2	.16
- Intransitive gestures (/36)	35.7 ± 1.5	34.9 ± 1.6	**.004**
- Transitive gestures (/36)	35.2 ± 2.0	34.9 ± 2.9	.79
Benson figure			
- Copy (17)	16.5 ± 0.8	16.6 ± 0.6	.92
- Recall (17)	12.8 ± 2.2	13.0 ± 2.5	.52
Free and Cued Recall Test			
- Free recall (/48)	35.6 ± 4.8	32.9 ± 5.5	.06
- Total recall (/48)	47.1 ± 1.5	46.4± 1.5	**.005**
- Delayed free recall (/16)	13.2 ± 2.1	13.0 ± 2.2	.88
- Delayed total recall (/16)	15.5 ± 1.8	15.6 ± 0.9	.70
Boston Naming Test (/30)	27.2 ± 2.0	27.2 ± 2.2	.93

Fluency tasks			
- Categories (Animals)	36.1 ± 10.3	36.3 ± 7.1	.82
- Letter (P)	24.7 ± 8.0	23.5 ± 6.5	.23

Figure 1

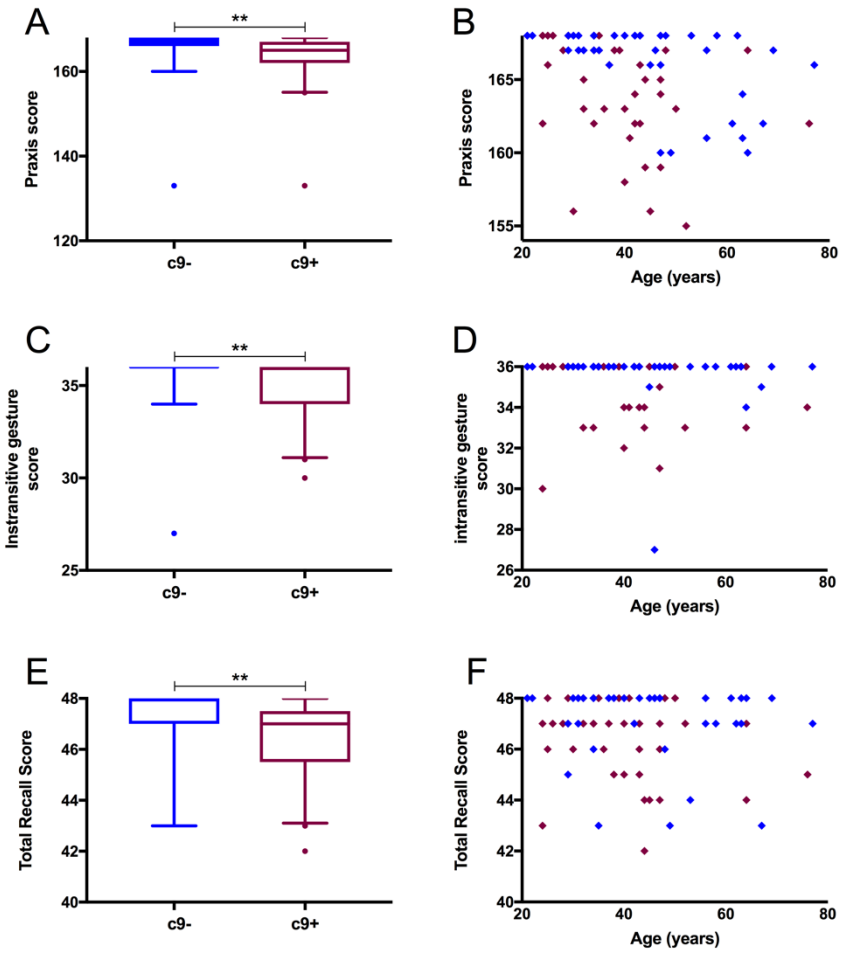
A
**
Praxis score
160
140
120
c9-
c9+
B
Praxis score
165
160
155
20
40
60
80
Age (years)
C
**
Instransitive gesture score
35
30
25
c9-
c9+
D
intransitive gesture score
36
34
32
30
28
26
20
40
60
80
Age (years)
E
**
Total Recall Score
48
46
44
42
40
c9-
c9+
F
Total Recall Score
48
46
44
42
40
20
40
60
80
Age (years)

Figure 2

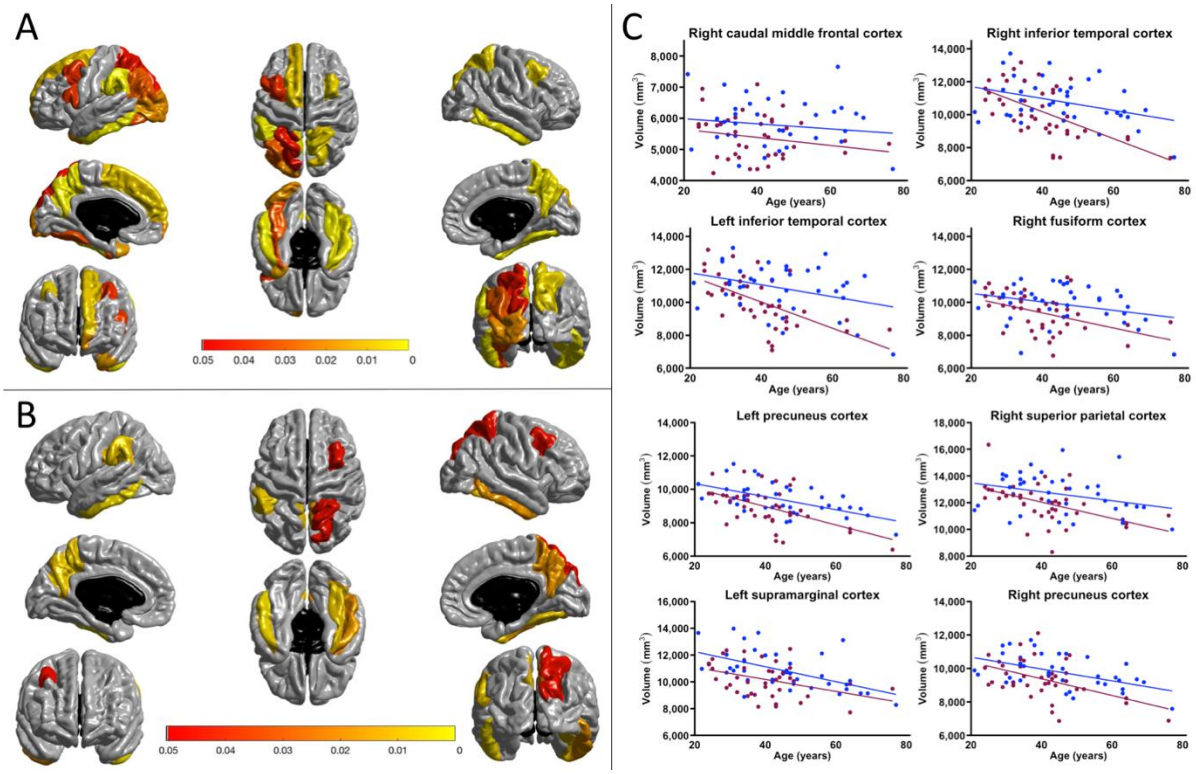
A
0.05 0.04 0.03 0.02 0.01 0
B
0.05 0.04 0.03 0.02 0.01 0
C
Right caudal middle frontal cortex
Right inferior temporal cortex
Left inferior temporal cortex
Right fusiform cortex
Left precuneus cortex
Right superior parietal cortex
Left supramarginal cortex
Right precuneus cortex
Volume (mm³)
Age (years)

Figure 3

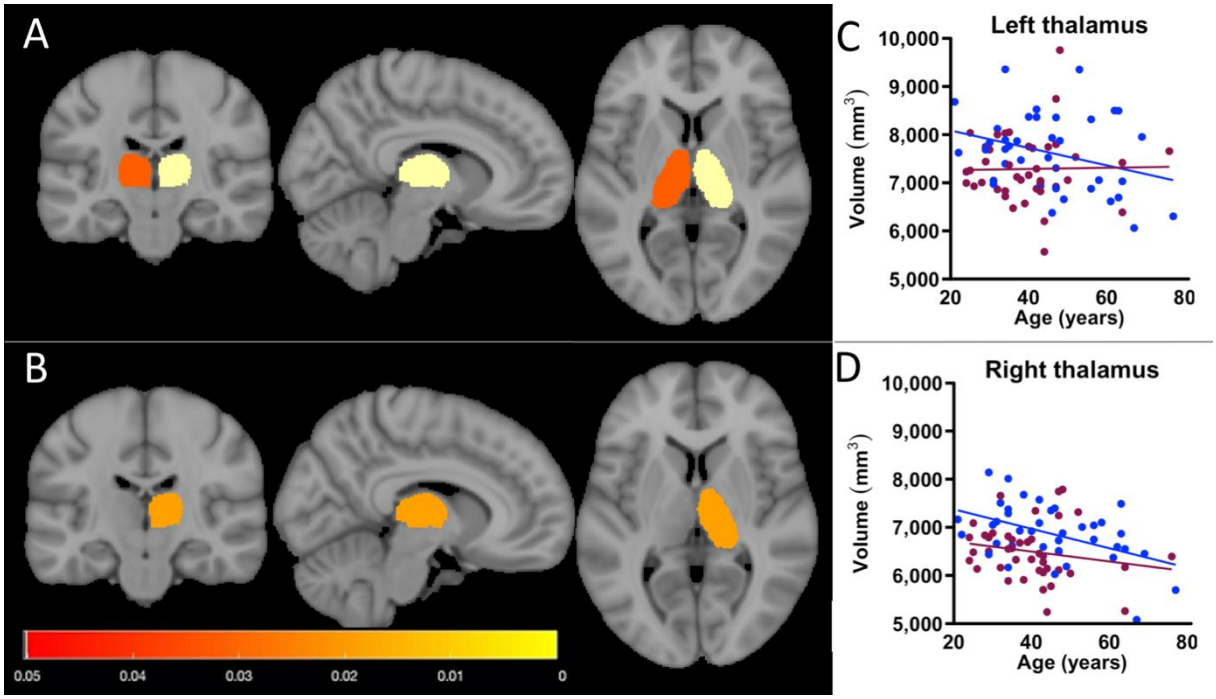
A
B
0.05
0.04
0.03
0.02
0.01
0
C
Left thalamus
Volume (mm3)
10,000
9,000
8,000
7,000
6,000
5,000
20
40
60
80
Age (years)
D
Right thalamus
Volume (mm3)
10,000
9,000
8,000
7,000
6,000
5,000
20
40
60
80
Age (years)

Figure 4

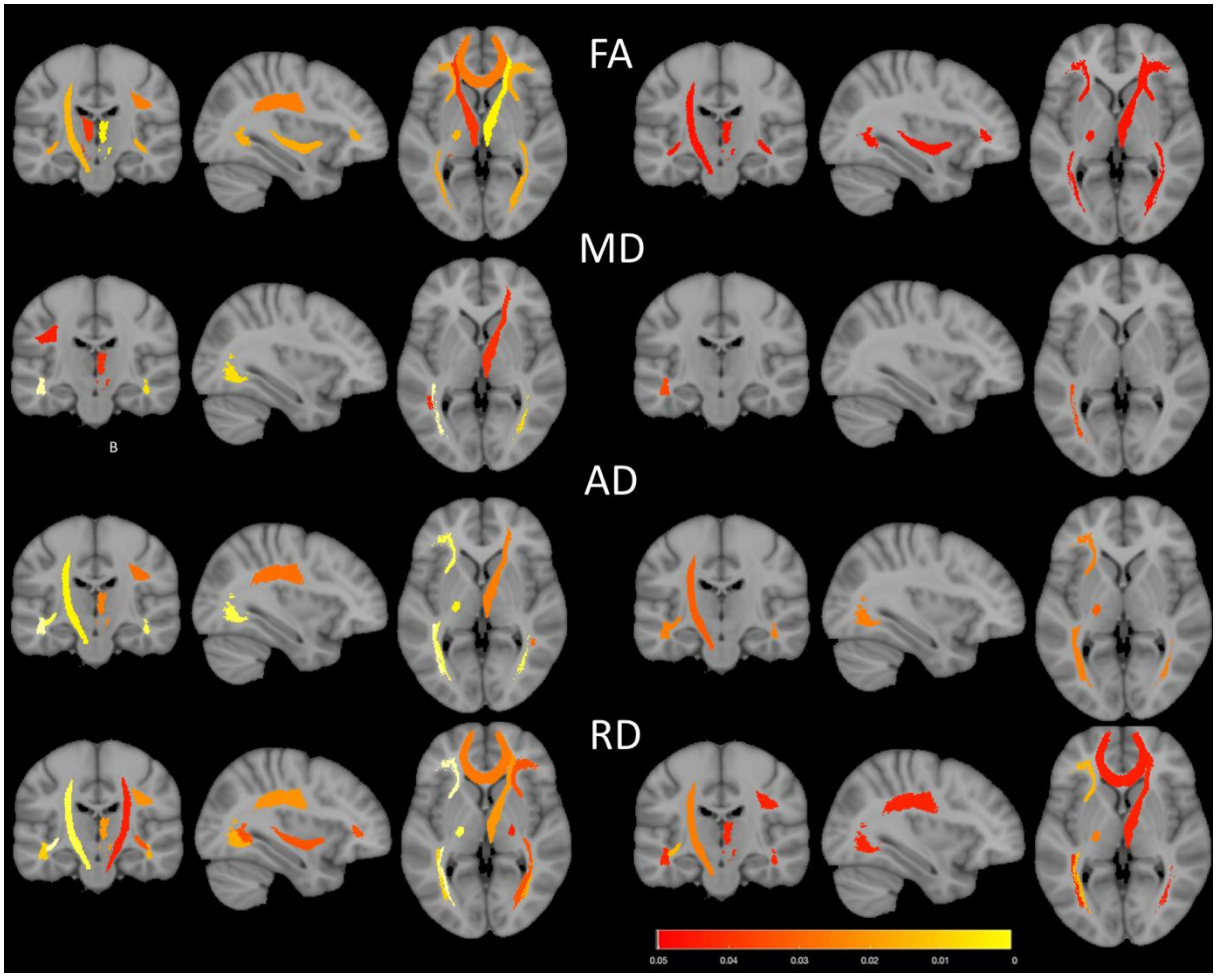

Supplementary materials

2 eMethod
2 eFigures
3 eTables

eMethod 1.

All the participants underwent a comprehensive neuropsychological and behavioral evaluation, based on internationally validated scales. disorders were assessed using the Frontal Behavioural Inventory (FBI), the Neuropsychiatric Inventory (NPI), the Frontal Behavioural scale, the Frontotemporal dementia Rating Scale (FRS), the CBI-R and Starskein apathy scale. Functional disability was assessed using the Frontal CDR and DAD scale (Disability Assessment for Dementia). Depression and anxiety were assessed using the STAI and BDI-II scale. All the participants also underwent a detailed neuropsychological battery evaluating global cognitive efficiency (Mini Mental State Examination (MMSE)[43], MATTIS dementia rating scale (MDRS[44]); executive functions (Frontal Assessment battery[45]); social cognition and theory of mind (Social Emotion Assessment [46]); episodic memory (Free and cued recall test); language (verbal fluencies, Boston Naming test) visuospatial processing (Benson figure copy) and gestural praxis. Gestural praxis were assessed with a shortened version of the Batterie d'Evaluation des Praxies[47] with 5 testing conditions: (a) manual dexterity, using imitation of finger configuration, (b) melokinetic apraxia, using motor programming and alternate gestures, (c) imitation of non-representational gestures, (d) pantomime of intransitive gestures, (e) pantomime of transitive gestures.

eMethod 2.

Parameters of 3DT1 sequence were as follow: spatial resolution = (1.1x1.1x1.1) mm3; TE/TR = 2.8-3ms/minimum; Bandwidth: 240-255 Hz. The 64 subjects imaged on a Siemens MR also underwent DTI with the following parameters: spatial resolution = (2x2x2.5) mm3; TE/TR = 90/7300ms; Bandwidth = 1580 Hz. Each DTI scan comprised 64 directions diffusion-weighted images (b value = 1000 s/mm2), 9 T2-weighted images (b value = 0 s/mm2) and a B0 field map.

eFigure 1: In c9+ subjects, real age and expected years to onset (based on the mean familial age at onset) showed strong correlation with high shared variance (Pearson correlation coefficient, $p < 0.0001$; $r^2 = 0.802$)

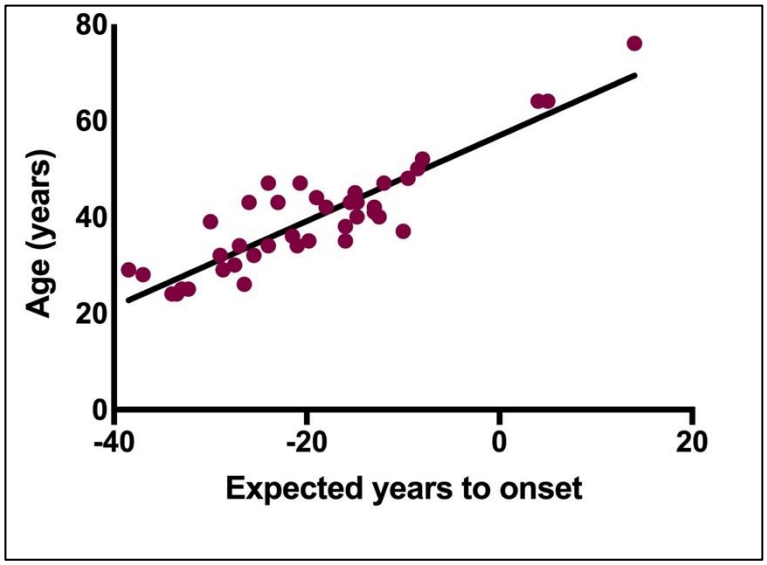

eFigure 2: Graphs of DTI metrics as a function of age in c9+ and c9- subjects. The exact position of x-values (age) is not provided, in order to prevent individual subjects from identifying their mutation status.

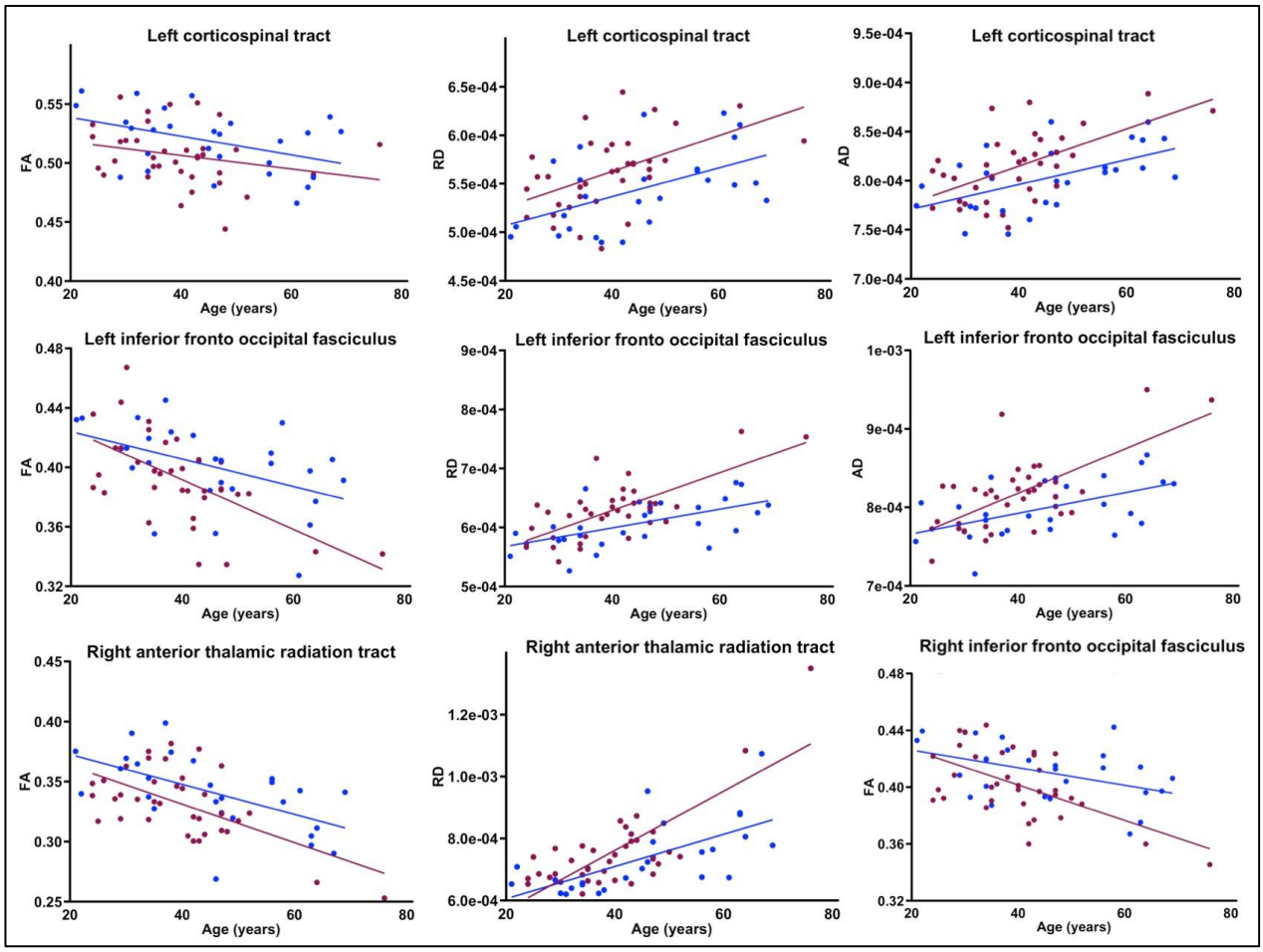

eTable 1: Effect of c9orf72 mutation on volume of cortical ROI, with age and sex as covariates. Uncorr.: uncorrected for multiple comparison; Corr.: corrected for multiple comparisons. Cortical ROI showing significant p-value after correction are shown in bold.

	c9orf72 mutation		
	Coefficient	Uncorr. p value	Corr. p value
Frontal lobe			
Left frontal pole	-76.8	0.016*	0.100
Left medial orbitofrontal	-199.8	0.096	0.211
Left lateral orbitofrontal	-185.1	0.113	0.240
Left pars orbitalis	-20.7	0.771	0.832
Left pars triangularis	-178.5	0.141	0.254
Left pars opercularis	-339.6	0.038*	0.155
Left rostral middle frontal	-208.3	0.536	0.675
Left caudal middle frontal	-381.2	0.039*	0.155
Left superior frontal	-1062.6	0.007*	0.053
Left precentral	-578.0	0.073	0.178
Right frontal pole	-28.1	0.502	0.649
Right medial orbitofrontal	-0.1	1.000	1.000
Right lateral orbitofrontal	-182.2	0.190	0.308
Right pars orbitalis	-138.5	0.058	0.155
Right pars triangularis	-109.8	0.394	0.558
Right pars opercularis	-278.4	0.066	0.166
Right rostral middle frontal	-635.8	0.053	0.155
Right caudal middle frontal	-490.1	0.005*	0.046*
Right superior frontal	-736.1	0.054	0.155
Right precentral	-476.9	0.086	0.201
Temporal lobe			
Left temporal pole	-212.6	0.015*	0.100
Left banks sts	-54.6	0.572	0.695
Left transverse temporal	-74.3	0.116	0.240
Left superior temporal	-372.3	0.177	0.294
Left middle temporal	-78.1	0.771	0.832
Left inferior temporal	-1155.7	<0.001*	0.005*
Left fusiform	-502.2	0.033*	0.155
Left entorhinal	-107.0	0.135	0.254
Left parahippocampal	-51.1	0.485	0.649
Right temporal pole	-111.4	0.157	0.274
Right banks sts	-2.0	0.980	0.994
Right transverse temporal	-15.3	0.694	0.800
Right superior temporal	-376.5	0.142	0.254
Right middle temporal	-178.0	0.547	0.676
Right inferior temporal	-924.3	0.002*	0.018*
Right fusiform	-833.8	<0.001*	0.008*
Right entorhinal	-48.6	0.506	0.649
Right parahippocampal	-115.9	0.059	0.155
Parietal lobe			
Left postcentral	-377.6	0.094	0.211
Left superior parietal	-692.9	0.045*	0.155
Left inferior parietal	-674.2	0.030*	0.155
Left precuneus	-711.3	<0.001*	0.008*
Left supramarginal	-972.2	<0.001*	0.008*
Left paracentral	-17.3	0.855	0.899
Right postcentral	-344.6	0.126	0.245
Right superior parietal	-854.9	0.005*	0.046*
Right inferior parietal	-649.2	0.058	0.155
Right precuneus	-677.8	0.002*	0.018*
Right supramarginal	-308.8	0.232	0.358
Right paracentral	-37.5	0.717	0.812

Occipital lobe			
Left lingual	-380.1	0.051	0.155
Left lateral occipital	-695.0	0.019*	0.107
Left cuneus	-137.2	0.051	0.155
Left pericalcarine	76.2	0.213	0.336
Right lingual	-132.0	0.501	0.649
Right lateral occipital	-590.6	0.051	0.155
Right cuneus	-117.5	0.163	0.277
Right pericalcarine	111.1	0.122	0.245
Cingulate gyrus			
Left rostral anterior cingulate	-74.8	0.349	0.505
Left caudal anterior cingulate	-38.2	0.728	0.812
Left isthmus cingulate	-142.3	0.059	0.155
Left posterior cingulate	-13.7	0.890	0.917
Right rostral anterior cingulate	-93.2	0.265	0.400
Right caudal anterior cingulate	18.5	0.859	0.899
Right isthmus cingulate	-32.6	0.670	0.785
Right posterior cingulate	42.8	0.589	0.702
Insula			
Left insula	-111.3	0.320	0.473
Right insula	-96.1	0.441	0.613

eTable 2: Effect of c9orf72 mutation on volume of subcortical structures, with age and sex as covariates. Uncorr.: uncorrected for multiple comparison; Corr.: corrected for multiple comparisons. Subcortical ROI showing significant p-value after correction is shown in bold.

	c9orf72 mutation		
	Coefficient	Uncorr. p value	Corr. p value
Left cerebellum cortex	-1043.4	0.385	0.629
Right cerebellum cortex	-687.2	0.570	0.790
Left ventral diencephalon	-31.3	0.704	0.810
Right ventral diencephalon	-7.8	0.915	0.935
Left putamen	-141.9	0.302	0.556
Right putamen	-176.0	0.176	0.420
Left pallidum	-84.6	0.065	0.342
Right pallidum	-57.1	0.186	0.420
Left caudate	-25.8	0.720	0.810
Right caudate	-6.6	0.935	0.935
Left accumbens area	-18.5	0.480	0.720
Right accumbens area	-24.5	0.309	0.556
Left amygdala	-20.2	0.659	0.810
Right amygdala	-71.1	0.151	0.420
Left thalamus proper	-383.0	0.022*	0.202
Right thalamus proper	-444.1	0.001*	0.010*
Left hippocampus	-161.6	0.100	0.360
Right hippocampus	-175.6	0.076	0.342

eTable 3: Effect of c9orf72 mutation on DTI metrics, with age and sex as covariates. Uncorr.: uncorrected for multiple comparison; Corr.: corrected for multiple comparisons. L.: left; R.: right. Tract with at least one DTI metric showing significant p-value after correction are shown in bold.

	FA			**MD**			**RD**			**AD**		
	Coeff. (x10)	Uncorr. p value	Corr. p value	Coeff. ($x10^3$)	Uncorr. p value	Corr. p value	Coeff. ($x10^4$)	Uncorr. p value	Corr. p value	Coeff. ($x10^4$)	Uncorr. p value	Corr. p value
L. anterior thalamic radiation	-0.120	0.035*	0.099	0.026	0.163	0.326	0.358	0.062	0.113	0.326	0.083	0.122
R. anterior thalamic radiation	-0.180	0.004*	0.049*	0.044	0.037*	0.229	0.596	0.011*	0.041*	0.546	0.015*	0.055
L. corticospinal tract	-0.165	0.008*	0.049*	0.006	0.531	0.758	0.279	0.002*	0.015*	0.209	0.004*	0.022*
R. corticospinal tract	-0.098	0.120	0.239	0.002	0.865	0.911	0.178	0.045*	0.099	0.124	0.086	0.122
L. cingulum cingulate gyrus	-0.230	0.105	0.239	0.022	0.334	0.542	0.506	0.053	0.105	0.410	0.065	0.119
R. cingulum cingulate gyrus	-0.171	0.246	0.378	-0.010	0.722	0.861	0.220	0.418	0.517	0.121	0.616	0.648
L. cingulum hippocampus	0.018	0.867	0.867	0.057	0.103	0.229	0.244	0.439	0.517	0.360	0.249	0.312
R. cingulum hippocampus	0.096	0.435	0.622	0.012	0.732	0.861	-0.024	0.970	0.970	0.024	0.924	0.924
Forceps major	-0.146	0.109	0.239	0.008	0.790	0.877	0.300	0.158	0.226	0.226	0.302	0.355
Forceps minor	-0.169	0.016*	0.052	0.001	0.958	0.958	0.277	0.016*	0.045*	0.187	0.067	0.119
L. inferior fronto occipital fasciculus	-0.163	0.010*	0.049*	0.023	0.077	0.229	0.334	<0.001*	0.008*	0.290	0.002*	0.015*
R. inferior fronto occipital fasciculus	-0.129	0.009*	0.049*	0.012	0.352	0.542	0.225	0.025*	0.062	0.189	0.058	0.119
L. inferior longitudinal fasciculus	-0.038	0.582	0.670	0.037	0.001*	0.027*	0.285	0.006*	0.040*	0.311	0.001*	0.015*
R. inferior longitudinal fasciculus	-0.081	0.235	0.378	0.041	0.005*	0.055	0.267	0.009*	0.041*	0.314	0.002*	0.015*
L. superior longitudinal fasciculus	-0.064	0.146	0.265	0.018	0.046*	0.229	0.159	0.080	0.133	0.167	0.053	0.119
R. superior longitudinal fasciculus	-0.136	0.015*	0.052	0.018	0.103	0.229	0.279	0.012*	0.041*	0.244	0.018*	0.055
L. uncinate fasciculus	-0.065	0.489	0.652	0.011	0.591	0.788	0.190	0.302	0.402	0.165	0.348	0.386
R. uncinate fasciculus	-0.030	0.800	0.842	-0.032	0.082	0.229	-0.116	0.503	0.559	-0.182	0.195	0.260
L. superior longitudinal fasciculus temporal	0.072	0.593	0.670	0.025	0.193	0.350	0.047	0.743	0.782	0.155	0.072	0.119
R. superior longitudinal fasciculus temporal	-0.062	0.603	0.670	0.034	0.088	0.229	0.174	0.109	0.168	0.232	0.019*	0.055

References

1. Folstein MF, Folstein SE, McHugh PR. "Mini-mental state". A practical method for grading the cognitive state of patients for the clinician. *J Psychiatr Res*. 1975;12(3):189-198.
2. Mattis S. Mental status examination for organic mental syndrome in the elderly patients. In: *Geriatrics Psychiatry: A Handbook for Psychiatrists and Primary Care Physicians*. New York: Grune & Stratton; 1976:77-121.
3. Dubois B, Slachevsky A, Litvan I, Pillon B. The FAB: a Frontal Assessment Battery at bedside. *Neurology*. 2000;55(11):1621-1626.
4. Funkiewiez A, Bertoux M, de Souza LC, Lévy R, Dubois B. The SEA (Social cognition and Emotional Assessment): a clinical neuropsychological tool for early diagnosis of frontal variant of frontotemporal lobar degeneration. *Neuropsychology*. 2012;26(1):81-90. doi:10.1037/a0025318.
5. Peigneux P, Van Der Linden M. Présentation d'une batterie neuropsychologique et cognitive pour l'évaluation de l'apraxie gestuelle. *Rev Neuropsychol*. 2000;10(2):311-362.